ÅSBRINK, S., KIHLBORG, L. & MALINOWSKI, M. (1988). *J. Appl. Cryst.* **21**, 960–962; erratum (1989). **22**, 380.
BAMBERG, J. (1987). Thesis, Saarbrücken, Germany.
BARBARA, T. M., GAMMIE, G., LYDING, J. W. & JONAS, J. (1988). *J. Solid State Chem.* **75**, 183–187.
BART, J. C. J. & RAGAINI, V. (1979). *Inorg. Chim. Acta*, **36**, 261–265.
BIRTILL, J. J. & DICKENS, P. G. (1978). *Mater. Res. Bull.* **13**, 311–316.
BROWN, I. D. (1981). *Structure and Bonding in Crystals*, Vol. II, edited by M. O'KEEFFE & A. NAVROTSKY, pp. 1–30. New York: Academic Press.
BROWN, I. D. & WU, K. K. (1976). *Acta Cryst.* B**32**, 1957–1959.
BUSING, W. R., MARTIN, K. D. & LEVY, H. A. (1974). *ORXFLS3*. Oak Ridge National Laboratory, Tennessee, USA.
CHOAIN, C. & MARION, F. (1963). *Bull. Soc. Chim. Fr.* p. 212.
COPPENS, P. (1968). *DATAPII*. SUNY, Buffalo, USA.
DEB, S. K. (1968). *Proc. R. Soc. London Ser. A*, **304**, 211–231.
DICKENS, P. G., BIRTILL, J. J. & WRIGHT, C. J. (1979). *J. Solid State Chem.* **28**, 185–193.
ESCRIBE-FILIPPINI, C., BEILLE, J., BOUJIDA, M., MARCUS, J. & SCHLENKER, C. (1989). *Physica*, C**162–164**, 427–428.
FLEMING, R. M. & CAVA, R. J. (1989). *Low-Dimensional Electronic Properties of Molybdenum Bronzes and Oxides*, edited by C. SCHLENKER, pp. 259–294. Dordrecht: Kluwer Academic Publishers.
FRÖHLICH, H. (1954). *Proc. R. Soc. London Ser. A*, **223**, 296–305.
GREENBLATT, M., MCCARROLL, W. H., NEIFELD, R., CROFT, M. & WASZCZAK, J. V. (1984). *Solid State Commun.* **51**, 671–674.
HORN, P. M. & GUIDOTTI, D. (1977). *Phys. Rev. B*, **16**, 491–501.
JOHNSON, C. K. (1976). *ORTEPII*. Report ORNL-5138. Oak Ridge National Laboratory, Tennessee, USA.
KATSCHER, H. & SCHRÖDER, F. (1987). Editors. *Gmelin Handbook of Inorganic Chemistry*, 8th ed., Mo Suppl., Vol. B3*a*, pp. 11–12. Berlin: Springer-Verlag.
KIERKEGAARD, P. (1964). *Ark. Kemi* **23**, 223–226.
KIVELSON, S. (1982). *Phys. Rev. B*, **25**, 3798–3821.
MIHÁLY, G., BEAUCHÊNE, P., MARCUS, J., DUMAS, J. & SCHLENKER, C. (1988). *Phys. Rev. B*, **37**, 1047–1050.
PEIERLS, R. E. (1955). *Quantum Theory of Solids*, p. 108. Oxford Univ. Press.
PIMENTEL, G. C. & MCCLELLAN, A. L. (1960). *The Hydrogen Bond*, p. 259. San Francisco: Freeman.
RAUB, C. J. (1988). *J. Less-Common Met.* **137**, 287–295.
RITTER, C., MÜLLER-WARMUTH, W. & SCHÖLLHORN, R. (1985). *J. Chem. Phys.* **83**, 6130–6138.
RITTER, C., MÜLLER-WARMUTH, W., SPIESS, H. W. & SCHÖLLHORN, R. (1982). *Ber. Bunsenges. Phys. Chem.* **86**, 1101.
SCHLENKER, C., DUMAS, J., ESCRIBE-FILIPPINI, C. & GUYOT, H. (1989). *Low-Dimensional Electronic Properties of Molybdenum Bronzes and Oxides*, edited by C. SCHLENKER, pp. 159–257. Dordrecht: Kluwer Academic Publishers.
SCHRÖDER, F. A. & WEITZEL, H. (1977). *Z. Anorg. Allg. Chem.* **435**, 247–256.
SLADE, R. C. T., HALSTEAD, T. K. & DICKENS, P. G. (1980). *J. Solid State Chem.* **34**, 183–192.
SU, W. P., SCHRIEFFER, J. R. & HEEGER, A. J. (1980). *Phys. Rev. B*, **22**, 2099.
TRAVAGLINI, G. & WACHTER, P. (1983). *Solid State Commun.* **47**, 217–221.
WHANGBO, M.-H. & CANADELL, E. (1989). *Acc. Chem. Res.* **22**, 375–381.
WILHELMI, K. A. (1969). *Acta Chem. Scand.* **23**, 419–428.
WILSON, J. A., DI SALVO, F. J. & MAHAJAN, S. (1975). *Adv. Phys.* **24**, 117–201.

Acta Cryst. (1993). B**49**, 967–973

Accurate Synchrotron Radiation $\Delta\rho$ Maps for K_2SiF_6 and K_2PdCl_6

BY J. R. HESTER, E. N. MASLEN AND N. SPADACCINI

Crystallography Centre, University of Western Australia, Crawley 6009, *Australia*

N. ISHIZAWA

Research Laboratory of Engineering Materials, Tokyo Institute of Technology, 4259 *Nagatsuta, Midori-Ku, Yokohama* 227, *Japan*

AND Y. SATOW

Faculty of Pharmaceutical Sciences, University of Tokyo, Hongo 7-3-1, *Bunkyo-ku, Tokyo* 113, *Japan*

(*Received* 1 *December* 1992; *accepted* 7 *June* 1993)

Abstract

Difference electron densities for the structurally isomorphic title compounds have been measured using 0.9 and 0.7 Å synchrotron radiation as well as Mo $K\alpha$ ($\lambda = 0.71069$ Å) radiation. The merits of using synchrotron radiation for such accurate electron density studies are confirmed. The noise level in the 0.9 Å K_2SiF_6 $\Delta\rho$ maps is low, and justifies confidence in physical properties predicted from the one-electron density. Similar $\Delta\rho$ features are present in both compounds. The redistribution of electron density indicated by the $\Delta\rho$ maps, which mainly reflects the effect of exchange interactions, does not support simple predictions from ionic and orbital models for the bonding in these structures. (I):

©1993 International Union of Crystallography
Printed in Great Britain – all rights reserved

Dipotassium hexafluorosilicate, K_2SiF_6, $Fm\bar{3}m$, cubic, $M_r = 220.27$, $a = 8.1419\ (3)$ Å, $V = 539.73\ (3)$ Å^3, $Z = 4$, $D_x = 2.711$ Mg m^{-3}, $\mu(0.9\ \text{Å}) = 3.919$, $\mu(0.7\ \text{Å}) = 1.909$, $\mu(\text{Mo } K\alpha) = 2.007$ mm^{-1}, $F(000) = 424$, $T = 293$ K, $R = 0.021$, $wR = 0.017$, $S = 4.458$ for 155 unique reflections measured with 0.9 Å data. (II): Dipotassium hexachloropalladate, K_2PdCl_6, $M_r = 397.3$, $Fm\bar{3}m$, cubic, $a = 9.7192\ (7)$ Å, $V = 918.1\ (2)$ Å^3, $Z = 4$, $D_x = 2.875$ Mg m^{-3}, $\mu = 8.8571$ mm^{-1}, $F(000) = 744$, $T = 293$ K, $R = 0.023$, $wR = 0.018$, $S = 5.041$ for 241 unique reflections at 0.9 Å.

Introduction

The high intensity of modern synchrotron X-ray sources enables accurate measurement of diffraction data for weak reflections, and thus reduces noise in electron density maps. Their tuneable wavelength helps us to measure structure factors for the stronger reflections more precisely. Measurement at two or more wavelengths enables the effects of extinction to be assessed from the ratios of intensities for the same Bragg reflection at those wavelengths.

The title compounds are structurally related to the important perovskite compounds. The unit cell can be considered as eight perovskite unit cells with alternate Pd or Si atoms removed. Previous studies of perovskites focused on more tractable compounds containing first-row transition metals, but many important perovskite compounds contain heavier atoms. Accurate measurement of $\Delta\rho$ for such compounds would help to extend our understanding of simple transition-metal perovskites to more complex structures. Accurate charge-density measurements of a lighter isomorph like K_2SiF_6 provide an independent check on the K_2PdCl_6 results.

K_2PdCl_6 was previously studied by Takazawa, Ohba & Saito (1988) and by DuBoulay & Maslen (1993). Intensity data for the study of Takazawa *et al.* (1988) were strongly affected by extinction. The reliability of the extinction corrections limits the accuracy of the results (Maslen & Spadaccini, 1993). Difficulties in correcting reliably for extinction were also experienced by DuBoulay & Maslen (1993). In order to assess the influence of extinction on previous work, very small crystal samples were used in the present study with the intention of reducing the effect of extinction. The high intensity of synchrotron radiation ensured that relatively weak reflections from the small crystals could be measured accurately.

K_2SiF_6 occurs in nature as hieratite. Its structure, first determined by Ketelaar (1935), indicated that with Si at the origin the K atom is at $\frac{1}{4},\frac{1}{4},\frac{1}{4}$ and F at $x,0,0$. The x(F) coordinate was redetermined by Loehlin (1984) to correct an anomalous Si—F bond length reported in the original paper. No electron density studies have been reported.

In order to compare the quality of electron densities obtainable from synchrotron and conventional sources, diffraction data were measured for a small crystal of K_2SiF_6 using the BL14A four-circle diffractometer facility at the Photon Factory synchrotron and a conventional X-ray tube source.

Experimental

(I) K_2SiF_6: Small colourless crystals were grown by standing a 1.0M KF solution in a glass volumetric flask for several weeks. They exhibited well developed {100} and {111} faces. Lattice parameters were determined from six reflections with $\theta = 26°$. The cell dimensions are in reasonable agreement with Loehlin's value of $a = 8.134\ (1)$ Å. Synchrotron beams with wavelengths $\lambda = 0.9000\ (1)$ and $0.7000\ (1)$ Å were monochromated with an Si(111) crystal, using a curved mirror to focus the X-rays (Satow & Iitaka, 1989). Mo $K\alpha$ radiation from the X-ray tube was monochromated by an oriented graphite monochromator in the equatorial setting using the 002 reflection.

Synchrotron intensity data were corrected for deadtime counting losses using the polynomial expansion:

$$R_L = R_o \sum_{i=0}^{5} C_i (R_o \tau)^i$$

where $C_0 = 1$, τ is the system deadtime, R_L is the true count rate and R_o the observed count rate. Values for τ and the coefficients C_i were determined by inverting the polynomial expansion of $R_o = R_L \exp(-R\tau)$ (Quintana, 1991) and verified by recording counts before and after inserting an absorber into beams with a range of intensities. The deadtime was determined to be 1.36 μs. Corrections were less than 1% for count rates less than 8500 counts s^{-1} and the polynomial correction was reliable (25% correction) up to count rates of 150 000 counts s^{-1}.

Very small specimens had been selected for study in order to ensure that the effects of extinction were minimal. The crystal habit and dimensions are illustrated in Fig. 1. The disadvantage of using such small crystals is that intensities for the weak reflections for the tube data, and to a lesser extent the 0.7 Å synchrotron data, were low, and the corresponding standard deviations were relatively high. This was offset to some degree by the high symmetry of the crystal, and the resulting large number of equivalents for general reflections. The intensity ratios for the 0.9 and 0.7 Å data sets did not change systematically with reflection intensity, confirming

that extinction was unimportant in these experiments. Neutral-atom form factors and anomalous-scattering factors were taken from *International Tables for X-ray Crystallography* (1974, Vol. IV). Other experimental details are listed in Table 1.* Computer programs *STARTX*, *DIFDAT*, *ABSORB*, *ADDATM*, *ADDREF*, *FC*, *CRYLSQ*, *BONDLA*, *FOURR*, *CHARGE*, *CONTRS*, *SLANT* and *PLOT* from the *Xtal*3.2 Crystallographic programs (Hall, Flack & Stewart, 1992), installed on DEC5000 workstation computers, were used in the analysis.

There is tolerable agreement between the coordinate and vibration parameters for the three data sets (Table 3), but there may be small systematic differences between the vibration amplitudes. Calculations based on the 0.9 Å data were the most reliable, weak reflections being more accurately determined using that radiation because of the higher beam intensity. The corresponding R value is the lowest for the three data sets. S is largest for the 0.9 Å data, as expected. The inadequacies of the free-atom model used in evaluating calculated structure factors (F_c), especially for reflections with $\sigma(F_o)$ small and $|F_o - F_c|$ significant, increase the value of the goodness of fit S. The more accurately determined the observed structure factors are, the larger S should be.

(II) K_2PdCl_6: Crystals, provided by DuBoulay, were irregular octahedra bounded by {111} and {100} faces. The specimens selected for synchrotron study had dimensions of approximately 100 μm (first data collection) and 50 μm (second data collection).

* Lists of structure factors have been deposited with the British Library Document Supply Centre as Supplementary Publication No. SUP 71262 (12 pp.). Copies may be obtained through The Technical Editor, International Union of Crystallography, 5 Abbey Square, Chester CH1 2HU, England.

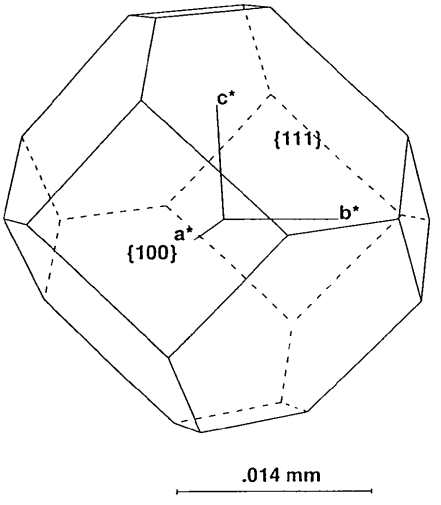

Fig. 1. K_2SiF_6 crystal shape for the synchrotron radiation experiment.

Table 1. K_2SiF_6 *experimental and refinement parameters*

	0.9 Å	0.7 Å	Mo $K\alpha$
Diffractometer	Rigaku	Rigaku	CAD-4
Monochromator	Silicon	Silicon	Graphite
Scan type	θ–2θ	θ–2θ	θ–2θ
θ scan width (°)	0.6	0.25	0.43 + 0.34tanθ
Maximum sin θ/λ (Å^{-1})	1.005	1.005	0.86
Number of reflections measured	4456	4644	2740
Transmission range	0.9136–0.9333	0.9568–0.9669	0.8945–0.9497
R_{int}	0.026	0.031	0.057
Number of independent reflections	155	155	99
R	0.021	0.031	0.038
wR	0.017	0.019	0.020
S	4.458	3.085	1.623
Maximum Δ/σ	4.5×10^{-5}	6.9×10^{-6}	6.1×10^{-5}
Maximum $\Delta\rho$ (e Å^{-3})	0.6	0.9	0.6
Minimum $\Delta\rho$ (e Å^{-3})	−0.6	−1.0	−0.8

Data were collected as for (I). Analysis of the first data set revealed that the peak intensities for some reflections were outside the range for which deadtime could be modelled accurately. A small inner sphere of reflections was remeasured at lower beam intensity to obtain more accurate measurements of these strong reflections. A second crystal sample was used for the latter data collection, as electron microscope photographs showed surface damage of the original sample. Dimensions determined by electron microscopy were used to correct for absorption before independent reflections were averaged. Equivalent reflection intensities in the inner-sphere data were inversely correlated to absorption-weighted mean path lengths ($\overline{T}$), indicating that secondary extinction was significant. An extinction-free structure-factor amplitude, F_k^2, was determined for all groups of equivalent reflections in this data set by extrapolating a linear fit of $\overline{T}$ *versus* $\log F_k^2$ to $\overline{T} = 0$. Values of $y = F_o^2/F_k^2$ were then plotted to provide a linear least-squares fit of $-\log y$ *versus* $F_k^2 G\overline{T}$, where G is the angle-dependent geometrical factor which includes polarization and Lorentz factors (see Maslen & Spadaccini, 1993). The form of this correction is suggested by the asymptotic behaviour of the Zachariasen (1967) equation

$$y = [1 + 2r^*\overline{T}G(s)F_k^2]^{-1/2}.$$

The significant positive gradient of $1.3\,(2) \times 10^{-4}$ was used to evaluate extinction corrections for each set of absorption-corrected equivalent reflections. The minimum y value of 0.43 for the {004} reflection is outside the range for which the Zachariasen expression is expected to be accurate. Equivalent data from the inner-sphere data set were then merged and combined with merged reflection data from the first data set. Refinement then proceeded as for (I). Refinement details are listed in Table 2. Extinction corrections were evaluated using *Mathematica*2.1 running on a Sun SparcStation (Wolfram, 1991).

Table 2. K_2PdCl_6 *experimental and refinement parameters*

	First data collection	Second data collection
Diffractometer	Rigaku	Rigaku
Monochromator	Silicon	Silicon
Scan type	θ–2θ	θ–2θ
θ scan width	0.75	0.25
Maximum sin θ/λ (Å^{-1})	1.007	0.469
	$-19 \le h,k,l \le 19$	$-8 \le h,k,l \le 8$
Number of reflections ($I > 0$)	7753	785
Absorption transmission range	0.5082–0.6907	0.7067–0.7671
$y_{min}(F^2)$	1.0	0.43
$R_{int}(F^2)$	0.0405	0.0527
Number of independent reflections	241	36

	Combined data
Data set merging agreement factor	0.0074
R	0.023
wR	0.018
S	5.041
Maximum Δ/σ	7.7×10^{-5}
Minimum, maximum $\Delta\rho$	−1.4, 0.4

Table 3. *Vibrational parameters* ($U_{ij} \times 10^3$ Å^2) *and* x (F/Cl)

K_2SiF_6

	0.9 Å	0.7 Å	Mo $K\alpha$
U_{11}(K)	24.9 (1)	23.7 (1)	24.0 (2)
U_{11}(Si)	17.5 (1)	17.7 (2)	16.3 (3)
U_{11}(F)	17.3 (3)	16.5 (4)	16.4 (6)
U_{22}(F)	36.6 (3)	36.0 (4)	35.3 (5)
x(F)	0.2067 (1)	0.2066 (1)	0.2060 (2)

K_2PdCl_6

	0.9 Å	Mo $K\alpha$ (DuBoulay & Maslen, 1993)	Mo $K\alpha$ (Takazawa *et al.*, 1988)
U_{11}(K)	36.5 (2)	35.9 (2)	35.6 (2)
U_{11}(Pd)	15.10 (5)	14.42 (8)	14.16 (5)
U_{11}(Cl)	16.2 (1)	16.1 (2)	15.7 (1)
U_{22}(Cl)	40.5 (2)	39.4 (2)	39.4 (2)
x(Cl)	0.23790 (4)	0.2379 (1)	0.23795 (5)

The refined structural parameters are compared with those of DuBoulay & Maslen (1993) and Takazawa *et al.* (1988) in Table 3. Agreement in general is less satisfying than that for K_2SiF_6, which was unaffected by extinction. While x(Cl) agrees well, the Pd U_{11} thermal vibration parameters differ significantly. Structure-factor residuals for the extinction-affected reflections contain several significant disagreements. The noticeable variation between the thermal parameters for the different data sets here may reflect uncertainties in the extinction corrections for either or all of the studies.

Atomic charges

Charges for the title compounds calculated by projecting the difference density $\Delta\rho$ onto atomic density basis functions (Hirshfeld, 1977) are listed in Table 4. K_2SiF_6 charges have little relationship to the formal values for the constituent atoms. The values

Table 4. *Atomic charges* (e)

K_2SiF_6

	0.9 Å	0.7 Å	Mo $K\alpha$
K	−0.05 (1)	−0.33 (2)	−0.20 (4)
Si	−0.03 (2)	0.09 (2)	−0.05 (5)
F	0.02 (1)	0.10 (2)	0.07 (3)

K_2PdCl_6

	0.9 Å	Mo $K\alpha$ (DuBoulay & Maslen, 1993)	Mo $K\alpha$ (Takazawa *et al.*, 1988)
K	0.2 (2)	0.33 (3)	0.34
Pd	0.7 (2)	0.32 (5)	0.14
Cl	−0.3 (2)	−0.16 (3)	−0.14

determined from the 0.9 Å K_2SiF_6 data set suggest that all the atoms are close to neutral in this structure. There is no indication of the substantial negative charge on the F atom that would be expected if electronegativity was an overriding factor in determining interatom electron transfer. The evidence strongly indicates that the K atom does not carry a positive charge. The Si atom is almost neutral, again in strong contrast with its formal value of +4.

On the other hand the measured atomic charges correlate with the closeness of the packing as indicated by the U_{ij} values. In general the vibration amplitudes are larger than those for the ideal perovskite structures, and the low charges in this structure are consistent with the view that strong positive atomic charges develop only on atoms which are packed tightly in structures (Maslen & Spadaccini, 1989).

The F atom, indicated as carrying a small positive charge, has the lowest U_{11} value for any atom in the structure. The vibration amplitudes imply that each SiF_6 unit can be regarded as an octahedral F_6 cage containing an Si atom that is bound, but not strained. The anisotropy of the F motion is consistent with that expected for libration of each semi-rigid SiF_6 unit about its centre-of-mass. The K atom, indicated as carrying the small but most strongly negative charge in all three analyses, has U_{ii} values larger than U_{11} for F and all U_{ii} for the Si atom. Thus, the negative sign of the K-atom charge is consistent with the view that it is not packed tightly in the structure.

The inadequacy of the naive interpretations of simple ionic models for K_2SiF_6 in terms of electron transfer is obvious from their erroneous predictions of atomic charge. Equating the formal values to physical charge transfer between atoms would impede rather than aid our understanding of the relationship between structure, charge density and physical properties in this compound.

Charges for K_2PdCl_6 have signs that are more consistent with formal atomic charges. As the charge calculations are relatively sensitive to the errors in the corrections to the extinction-affected reflections,

the present results have relatively high uncertainties. Although relative sizes are broadly in keeping with the formal values, their magnitudes are smaller.

Electron density

Figs. 2(*a*) and 2(*b*) show difference maps for the (110) plane calculated from the K_2SiF_6 0.9 Å and K_2SiF_6 Mo $K\alpha$ data, respectively. The noise reduction due to improved accuracy of intensities of the weak reflections measured with synchrotron radiation is obvious in Fig. 2(*a*). The corresponding $\Delta\rho$ map for the 0.7 Å data closely resembles Fig. 2(*a*), but with more noise, reflecting the higher R value for that set. The difference electron density in regions away from the atomic nuclei in Fig. 2(*a*) is low and the map contains no sharp gradients in those regions, as expected from fundamental considerations because the Schrödinger equation predicts that ρ will not change rapidly where the electrostatic potential is slowly varying. There is a sea of positive electron density between the atoms in Fig. 2(*a*), but this is defined less clearly than those in more closely packed structures.

Electron density is depleted in the structural cavities, a phenomenon which is consistent with the depletion or accumulation of electron density observed in structural cavities in perovskite and related structures (*e.g.* Buttner & Maslen, 1992; Maslen & Spadaccini, 1989, and references therein). The strongest depletion occurs at the intersection of the K—K and Si—Si vectors which has unit-cell coordinate $(\frac{1}{4},\frac{1}{4},0)$, corresponding to the lower-right corner of Fig. 2. Smaller depletions occur in structural cavities associated with the midpoints of F—F vectors $[(0,0,\frac{1}{2})$, upper-left corner of Fig. 2] and K—K vectors $[(\frac{1}{4},\frac{1}{4},\frac{1}{2})$, upper-right corner of Fig. 2]. The relative strength of depletion is correlated to the relative size of the atoms surrounding the structural cavities.

A consistent but perhaps unexpected feature in all maps is the anisotropic shape of the electron distribution around the K atom. Electron density is strongly depleted near the K nucleus along the K—Si vectors on the side closest to Si. Electron density is transferred to the opposite side of the K atom. There is a corresponding but less-marked depletion close to the Si nucleus along the K—Si vectors. A low-temperature ($T = 100$ K) experiment was conducted on K_2SiF_6 using Mo $K\alpha$ radiation to investigate the possibility that these features were caused by anharmonicity in the K atom's thermal vibrations. Electron densities near the K atom calculated from the low-temperature data were similar to those in the room-temperature maps, indicating that the lobes around K represent redistribution of electron density due to bonding in this structure.

Fig. 3 shows the (110) plane for K_2PdCl_6. The maps display little short-range fluctuation. This low 'noise' is consistent with the K_2SiF_6 study. Atomic core regions are characterized by strong depletion of electron density. No correspondingly large accumulations of electron density are observed. The electrons have instead moved into a broad interatomic sea, punctuated by depletions of electron density at the midpoints of interatomic K—K, Pd—Pd and K—Pd vectors. The depletion associated with the K—Pd vector (lower centre of figure) is noticeably weaker than those between atoms of the same type.

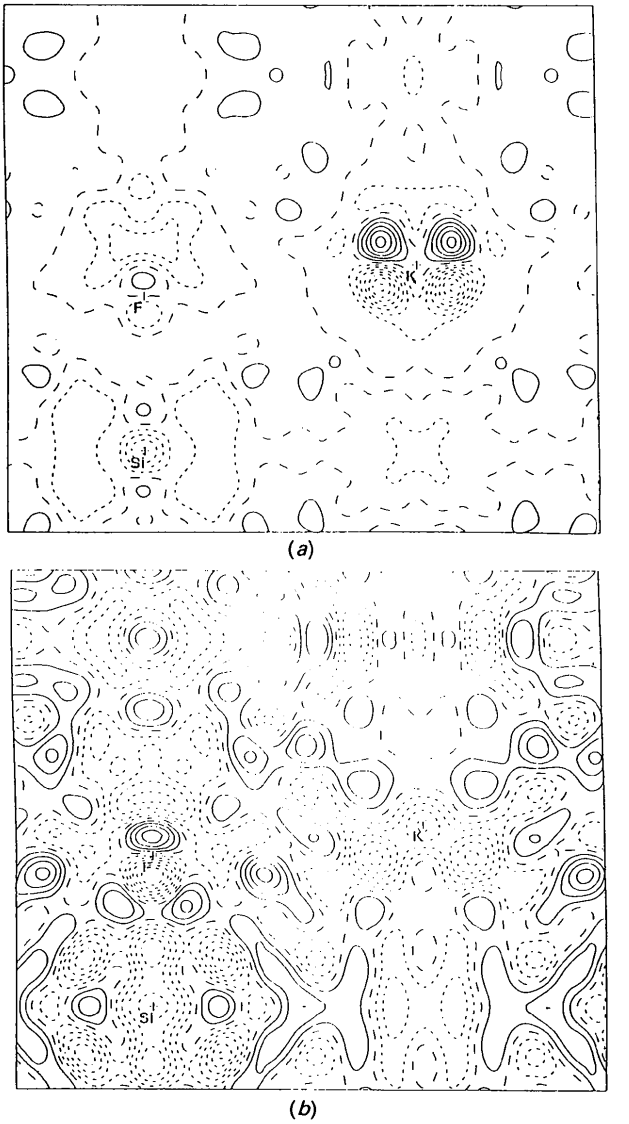

Fig. 2. (110) $\Delta\rho$ sections in K_2SiF_6 for (*a*) 0.9 Å synchrotron radiation and (*b*) Mo $K\alpha$ radiation. Contour interval 0.1 e Å^{-3}, borders 6.2 × 5.7 Å. Solid lines – positive $\Delta\rho$, dotted – negative, dashed – zero.

The asymmetric K electron distribution is topographically similar to that observed in K_2SiF_6. The effect is masked to some extent by stronger overall depletion of density around the K nucleus. Similar $\Delta\rho$ topographies are present in the results of Takazawa *et al.* (1988) and DuBoulay & Maslen (1993). Strong depletions have also been observed around atomic nuclei in K_2PdCl_4 (Hester, Maslen, Spadaccini, Ishizawa & Satow, 1993), for which no difficulty was encountered in correcting for extinction. Such strong depletion of valence density which overlaps with atomic cores is the expected result of the exchange terms in the wavefunctions for the system. As noted by Maslen & Spadaccini (1993) conventional least-squares refinement of extinction may reduce the polarity observed for structures with cations heavier than the anions, because the exchange depletion of density for heavy cations is masked by a bias in the extinction corrections determined by least-squares refinement of the structure.

The tetrahedral geometry of the antisymmetric feature around the K atom is obviously related more strongly to the K–cation interactions than to the K–halide interactions. That is, the depletions of electron density along the K–cation vectors are those expected for exchange depletion of closed inner subshells which overlap with the valence electrons of the neighbouring atom. Note that in the K_2SiF_6 case, the tetrahedral geometry of this antisymmetric feature cannot be constructed from K-atom 4*s* valence orbitals and low-lying vacant 3*d* orbitals only. Its geometry is that of a *p–d* orbital product and its radial dependence is best explained by a transfer of electrons involving the filled 3*p* and the vacant 3*d* subshells.

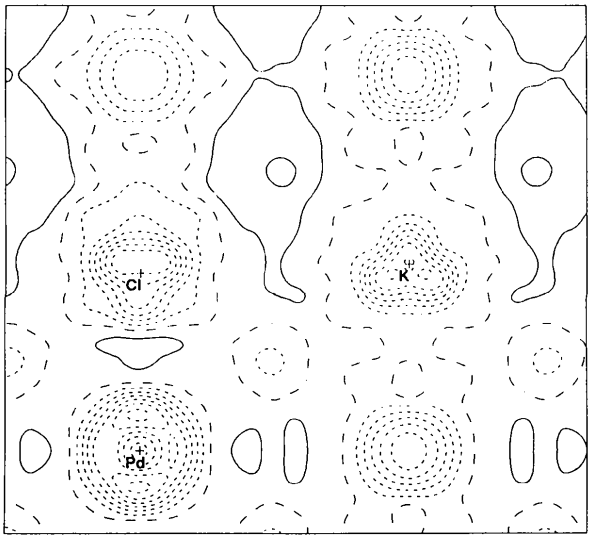

Fig. 3. (110) $\Delta\rho$ section in K_2PdCl_6 from 0.9 Å synchrotron radiation. Borders 7.4 × 6.8 Å, contour interval 0.2 e Å^{-3}.

The large size of this feature in the $\Delta\rho$ map indicates that there is significant interaction between the K and the other cation which are second-nearest neighbours, notwithstanding the relatively large distance between K and the cation [K—Si 3.5255 (1), K—Pd 4.2085 (1) Å]. The exchange depletion for K, which has a filled 3*p* subshell, is greater than that for Si, which has the partly filled $3p^2$ configuration. No lobes of electron accumulation analogous to those around K exist near Si because there are no low-lying vacant states of appropriate symmetry. Any concentration of electrons in 3*p* states for Si by the Si—F bonding is largely offset by depletion originating in nonbonding interactions between the Si and other atoms in the structure.

Serious limitations in some orbital models of atomic interactions are revealed by these electron density maps. The suspect models assume that features in the $\Delta\rho$ map will be dominated by concentration of orbital density associated with the nearest-neighbour bonding interactions. The cation–K second-nearest-neighbour interactions, where the exchange term is antibonding, are far more significant than those models suggest.

Note, however, that the fact that the larger features in the $\Delta\rho$ map are predominantly due to second-nearest neighbours does not imply that these interactions make a greater contribution to the bonding energy than nearest-neighbour interactions. The bonding energy is predominantly due to the promolecule contribution, represented by a flat difference map. That energy contribution is first order, whereas $\Delta\rho$ terms contribute only at second order to bonding energy. The contribution of the nearest-neighbour atoms is greater than those of second-nearest-neighbour interactions, because atomic overlap energy falls off exponentially with distance.

The contributions of computer programs by their authors R. Alden, G. Davenport, R. Doherty, W. Dreissig, H. D. Flack, S. R. Hall, J. R. Holden, A. Imerito, R. Merom, R. Olthof-Hazenkamp, M. A. Spackman, N. Spadaccini and J. M. Stewart to the *Xtal*3.0 system (Hall & Stewart, 1990), used extensively in this work, is gratefully acknowledged. The authors also acknowledge the support of the Australian Research Council and of the Japanese Ministry of Education.

Note added in proof: A further experiment on K_2PdCl_6 using 0.7 Å synchrotron radiation has been conducted. There is very close agreement between the electron density maps and vibrational parameters for 0.7 and 0.9 Å radiation. A structure-factor list-

ing, electron density map and listing of refined parameters have been deposited.

References

BUTTNER, R. & MASLEN, E. N. (1992). *Acta Cryst.* B**48**, 764–769.

DUBOULAY, D. & MASLEN, E. N. (1993). *Acta Cryst.* In preparation.

HALL, S. R., FLACK, H. D. & STEWART, J. M. (1992). Editors. *Xtal*3.2 *Reference Manual.* Univs. of Western Australia, Australia, and Maryland, USA.

HALL, S. R. & STEWART, J. M. (1990). Editors. *Xtal*3.0 *Reference Manual.* Univs. of Western Australia, Australia, and Maryland, USA.

HESTER, J. R., MASLEN, E. N., SPADACCINI, N., ISHIZAWA, N. & SATOW, Y. (1993). *Acta Cryst.* B**49**, 842–846.

HIRSHFELD, F. L. (1977). *Isr. J. Chem.* **16**, 198–201.

KETELAAR, J. A. A. (1935). *Z. Kristallogr.* **92**, 155–156.

LOEHLIN, J. H. (1984). *Acta Cryst.* C**40**, 570.

MASLEN, E. N. & SPADACCINI, N. (1989). *Acta Cryst.* B**45**, 45–52.

MASLEN, E. N. & SPADACCINI, N. (1993). *Acta Cryst.* A**49**, 661–667.

QUINTANA, J. P. (1991). *J. Appl. Cryst.* **24**, 261–262.

SATOW, Y. & IITAKA, Y. (1989). *Rev. Sci. Instrum.* **60**, 2390–2393.

TAKAZAWA, H., OHBA, S. & SAITO, Y. (1988). *Acta Cryst.* B**44**, 580–585.

WOLFRAM, S. (1991). *Mathematica: A System For Doing Mathematics by Computer.* Redwood City: Addison-Wesley.

ZACHARIASEN, W. H. (1967). *Acta Cryst.* A**23**, 558–564.

Acta Cryst. (1993). B**49**, 973–980

Synchrotron X-ray Study of the Electron Density in α-Al_2O_3

BY E. N. MASLEN, V. A. STRELTSOV* AND N. R. STRELTSOVA

Crystallography Centre, University of Western Australia, Nedlands 6009, *Australia*

N. ISHIZAWA

Research Laboratory of Engineering Materials, Tokyo Institute of Technology, 4259 *Nagatsuta, Midori-Ku, Yokohama* 227, *Japan*

AND Y. SATOW

Faculty of Pharmaceutical Sciences, University of Tokyo, Hongo 7-3-1, *Bunkyo-ku, Tokyo* 113, *Japan*

(*Received* 21 *December* 1992; *accepted* 1 *July* 1993)

Abstract

Structure factors for corundum, α-Al_2O_3, have been measured using 0.7 and 0.9 Å synchrotron radiation as well as Mo $K\alpha$ ($\lambda = 0.71069$ Å) radiation. The stronger structure factors from two sets of synchrotron data and three sets of Mo $K\alpha$ tube data for two small crystals are remarkably consistent. In analysing those data, extinction corrections evaluated by minimizing differences between equivalent reflection intensities were compared with those from the more common procedure of least-squares determination of the extinction parameters as a part of the structure refinement. Difference electron densities evaluated with extinction corrections from equivalent reflection intensities are more consistent than those which optimize $|F_o|$ *versus* $|F_c|$ agreement. Approximate symmetry in the concordant densities is related more closely to the Al—Al geometry than to nearest neighbour Al—O interactions. Space group $R\bar{3}c$, hexagonal, $M_r = 101.96$, $a = 4.7540$ (5), $c = 12.9820$ (6) Å, $V = 254.09$ (6) Å^3, $Z = 6$, $D_x = 3.997$ Mg m^{-3}, $\mu(0.9\text{ Å}) = 2.361$, $\mu(0.7\text{ Å}) = 1.097$, μ(Mo $K\alpha$) = 1.139 mm^{-1}, $F(000) = 300$, $T = 293$ K, $R = 0.024$, $wR = 0.030$, $S = 4.84$ for the unique 0.7 Å synchrotron reflection data.

Introduction

The corundum α-Al_2O_3 structure can be classified as an archetypal special class within the important perovskite ABX_3 series. The series as a whole includes many compounds with a wide variety of physical properties. Even the metal sesquioxides with the α-Al_2O_3 structure have some markedly different properties. A detailed understanding of the structure and electron density for the parent α-Al_2O_3 compound is a prerequisite to classifying physical property/structure relationships for the perovskite series as a whole.

Over the past decade the electron density in single crystals of α-Al_2O_3 has been measured in X-ray diffraction analyses by Lewis, Schwarzenbach & Flack (1982), Tsirelson, Antipin, Gerr, Ozerov &

* Author to whom correspondence should be addressed.

© 1993 International Union of Crystallography
Printed in Great Britain – all rights reserved